# Premature termination codons in *PRPF31* cause retinitis pigmentosa via haploinsufficiency due to nonsense-mediated mRNA decay

Thomas Rio Frio,[1] Nicholas M. Wade,[1] Adriana Ransijn,[1]
Eliot L. Berson,[2] Jacques S. Beckmann,[1,3] and Carlo Rivolta[1]

[1]Department of Medical Genetics, University of Lausanne, Lausanne, Switzerland.
[2]Berman-Gund Laboratory for the Study of Retinal Degenerations, Harvard Medical School, Boston, Massachusetts, USA. [3]Service of Medical Genetics, Centre Hospitalier Universitaire Vaudois, Lausanne, Switzerland.

**Dominant mutations in the gene encoding the mRNA splicing factor PRPF31 cause retinitis pigmentosa, a hereditary form of retinal degeneration. Most of these mutations are characterized by DNA changes that lead to premature termination codons. We investigated 6 different *PRPF31* mutations, represented by single-base substitutions or microdeletions, in cell lines derived from 9 patients with dominant retinitis pigmentosa. Five of these mutations lead to premature termination codons, and 1 leads to the skipping of exon 2. Allele-specific measurement of *PRPF31* transcripts revealed a strong reduction in the expression of mutant alleles. As a consequence, total PRPF31 protein abundance was decreased, and no truncated proteins were detected. Subnuclear localization of the full-length PRPF31 that was present remained unaffected. Blocking nonsense-mediated mRNA decay significantly restored the amount of mutant *PRPF31* mRNA but did not restore the synthesis of mutant proteins, even in conjunction with inhibitors of protein degradation pathways. Our results indicate that most *PRPF31* mutations ultimately result in null alleles through the activation of surveillance mechanisms that inactivate mutant mRNA and, possibly, proteins. Furthermore, these data provide compelling evidence that the pathogenic effect of *PRPF31* mutations is likely due to haploinsufficiency rather than to gain of function.**

## Introduction

Retinitis pigmentosa (RP) is a hereditary disease that causes progressive degeneration of the retina and leads in many cases to complete loss of sight. Clinically, RP is characterized by night blindness, which typically occurs at a young age. This is followed by progressive reduction of the visual field, generally from the mid-periphery to the far-periphery and then to the center, as a consequence of the gradual degeneration of both rod and cone photoreceptors. Electroretinograms (ERGs), which measure the electrical response of the retina to flashes of light, show that retinal responses are reduced and delayed in early life in patients with RP. As the disease progresses, ERGs decline in amplitude, retinal arterioles become attenuated, and the fundi usually show intraretinal pigment around the mid-periphery, after which the condition was named (1). Randomized trials have shown that the average rate of progression of this condition was slowed in patients taking a daily dose of vitamin A as retinyl palmitate (2) and that, among those patients starting vitamin A supplementation for the first time, docosahexaenoic acid intake provided additional benefit for 2 years (3). Further observations over 4 years suggested that an oily fish diet enriched in omega-3 fatty acids, rather than docosahexaenoic acid supplementation, can further slow this condition (3). Currently, the biochemical bases of these beneficial effects remain unclear. This disease is usually transmitted as a simple Mendelian trait (dominant, recessive, or X-linked), although some exceptions exist (4, 5). So far, more than 80 different loci causing RP have been cloned or mapped (6), among which is *PRPF31*, a gene associated with dominant RP and that encodes a pre-mRNA splicing factor.

*PRPF31* differs from most RP genes because it is ubiquitously expressed and it is essential for general cell metabolism and survival (7). Nonetheless, it can be responsible for a disease that is restricted to the retina only, because heterozygous patients carrying *PRPF31* mutations suffer from RP with no associated syndromes (8, 9). The role of *PRPF31* in the etiology of dominant RP is very likely linked to its main function in the mRNA splicing process, because 4 other essential pre-mRNA splicing factors and key components of the spliceosome have also been found to be involved in this disease (10–13).

Nonsense-mediated mRNA decay (NMD) is a widespread cellular process that proofreads nascent mRNA transcripts and destroys those that bear premature termination codons (PTCs) before they are actually translated into truncated and potentially harmful proteins (14, 15). Similar to genomic deletions, most mutations producing PTCs behave as null alleles, because their corresponding mRNA is quickly degraded. However, if the PTC produced by the mutation occurs in the last exon of a given gene, the mutant mRNA is insensitive to NMD and is thought to be translated into a truncated protein (14, 15). There are many examples of how NMD plays an essential role in human hereditary conditions, e.g., by inactivating PTC-containing alleles and by modifying the clinical phenotype or inheritance pattern of the

**Nonstandard abbreviations used:** ERG, electroretinogram; NMD, nonsense-mediated mRNA decay; NMTR, nonsense-mediated translational repression; PTC, premature termination codon; RP, retinitis pigmentosa.

**Conflict of interest:** The authors have declared that no conflict of interest exists.

**Citation for this article:** *J. Clin. Invest.* **118**:1519–1531 (2008). doi:10.1172/JCI34211.

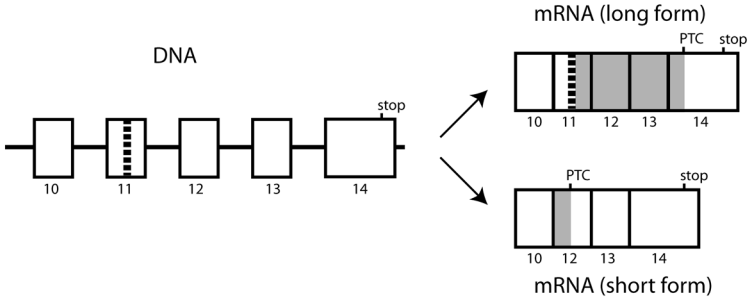


**Figure 1**
Effect of the *PRPF31* c.1115_1125del mutation on its own transcripts. Mutant *PRPF31* alleles carrying this mutation (vertical dotted bar) result in either a long mRNA form, which bears the deletion and a PTC just before the natural termination codon (stop) in exon 14, or a short mRNA form, in which exon 11 is skipped during splicing and a PTC is created in exon 12. The gray areas indicate the portion of the transcripts that have an out-of-phase reading frame. The drawing is not to scale.

disease (16, 17). One classic example is represented by dominant and recessive β-thalassemia (18). In this condition, all alleles producing PTCs in exons 1 or 2 lead to unstable mRNA and to a complete lack of β-globin in homozygotes (recessive form, where heterozygotes are healthy), whereas PTCs located in the last exon (dominant form) are also pathogenic in heterozygotes, because these mutations are insensitive to NMD and produce truncated dominant-negative forms of β-globin.

We performed a PubMed scan of the existing literature and found 40 different *PRPF31* mutations. Three of these 40 mutations (p.Ala216Pro, p.Ala192Glu, and p.Thr138Lys) are clear-cut missense changes (9, 10), whereas 2 others (p.Glu183_Met193dup and p.His111_Ile114del) cause the insertion or deletion of a few amino acids to the canonical polypeptide chain (10, 19). The remaining 35 mutations are either large chromosomal deletions (6 of 35) or are mutations that lead to PTCs (29 of 35) and therefore are predicted to undergo NMD (9, 10, 20–30). Of the latter mutations, c.1115_1125del, which is characterized by the deletion of 11 nucleotides in the middle of exon 11, deserves particular mention. This microdeletion was found in a very large family with dominant RP and was initially thought to be an NMD-insensitive allele because, based on in silico analyses, it would create a PTC in exon 14, the last *PRPF31* exon (10). Subsequent data have suggested that this mutation could inactivate an exonic splicing enhancer and thus promote the skipping of the entire exon 11 during mRNA splicing (30) and result in an out-of-phase PTC in exon 12. Accordingly, the c.1115_1125del change is expected to trigger NMD in the same way as all other PTC mutations (30) (Figure 1).

Here we investigate the functional bases of 6 different PTC-containing *PRPF31* mutations that recapitulate a substantial portion of the pathogenic variants detected thus far in patients with *PRPF31*-associated RP. To accurately reflect the natural situation, we took advantage of the ubiquitous expression of *PRPF31* and analyzed the endogenous allelic mRNA and protein levels in lymphocyte cell lines derived from patients, thereby avoiding classic techniques based on the insertion of exogenous mutations by cell transfection and analysis of foreign DNA. We demonstrated that these *PRPF31* mutations result in null alleles and decreased amounts of functional proteins. These findings have implications for most RP mutations linked to splicing factors, the physiological basis for the disease, and its clinical treatment.

## Results

*Clinical evaluation of patients.* This study included 9 patients with dominant RP with known mutations in the *PRPF31* gene (Table 1). Ophthalmologic evaluations for individuals AG0293, AG0305, and AG0307 were reported previously (31). The clinical findings for the remaining 6 patients at their initial visit are summarized in Table 2. All patients had ERG findings typical of this condition, with reductions in both rod-dominated 0.5-Hz responses and cone-isolated 30-Hz responses. In common with other forms of RP, a similar pattern of field loss, presence of cataracts in some cases, and typical bone spicule pigment around the periphery was observed in 5 of 6 of these patients. Of interest was patient 14523, who had a lower reduction in ERG amplitudes recorded from both eyes than did the 5 other patients who presented at a younger age. This patient also showed no bone spicule pigment.

**Table 1**
Mutations and their effects at the mRNA level in lymphoblastoid cell lines derived from patients with RP

| Cell line | Mutation | | Effect | PTC in exon | Predicted protein size |
|---|---|---|---|---|---|
| 14523 | IVS2+1delG | c.177+1delG | Skipping of exon 2, containing the natural AUG start codon | ND | Multiple |
| 14686 | Leu107Val (CTG>GTG) | c.319C>G | Partial skipping of exon 4, frameshift | 7 | 195 aa |
| 14266 | IVS4-2A>G | c.323-2A>G | Skipping of exon 5, frameshift | 6 | 119 aa |
| 12688, 13190 | IVS8-2A>G | c.856-2A>G | Partial retention of intron 8, frameshift | 10 | 331 aa |
| 14284 | Arg293(34-bp del) | c.877_910del | Frameshift | 10 | 308 aa |
| AG0293, AG0305, AG0307 | Arg372(11-bp del) | c.1115_1125del | Short form: skipping of exon 11, frameshift (86% of transcripts) | 12 | 387 aa |
| | | | Long form: exon 11 with deletion maintained, frameshift, stop codon in last exon (14% of transcripts) | 14 | 469 aa |

ND, not determined.

**Table 2**
Clinical features of patients examined for this study

| Patient | Age | Sex | Eye | VA | VF area | ERG 0.5 Hz[A] | ERG 30 Hz[B] | PSC | BSP |
|---|---|---|---|---|---|---|---|---|---|
| 14523 | 46 | M | OD | 20/25 | 12808 | 13.2 | 14.7 | N | N |
| | | | OS | 20/25 | 13171 | 17.8 | 16.2 | N | N |
| 14686 | 25 | F | OD | 20/30 | 5715 | 0.65 | 0.65 | N | Y |
| | | | OS | 20/30 | 5014 | NA | 0.65 | N | Y |
| 14266 | 34 | M | OD | 20/80 | 69 | 3.75 | 0.67 | Y | Y |
| | | | OS | 20/80 | 68 | 3.52 | 1.23 | Y | Y |
| 12688 | 23 | F | OD | 20/30 | 2248 | 4.7 | 3.34 | N | Y |
| | | | OS | 20/30 | 3772 | 6.6 | 4.02 | N | Y |
| 13190 | 33 | F | OD | 20/30 | 14671 | 4.5 | 1.46 | Y | Y |
| | | | OS | 20/30 | 13188 | 4.2 | 1.71 | Y | Y |
| 14284 | 40 | F | OD | 20/40 | 333 | 1.7 | 0.59 | Y | Y |
| | | | OS | 20/30 | 333 | 1.6 | 0.73 | Y | Y |

OD, right eye; OS, left eye; VA, best-corrected Snellen visual acuity; VF, total visual field area in degrees squared to a V-4e white stimulus in the Goldmann perimeter (normal values ≥ 11399 degrees squared); NA, not available; PSC, posterior subcapsular cataract; BSP, bone spicule pigmentation; Y, present; N, not present. [A]Normal values, ≥350 μV. [B]Normal values, ≥50 μV.

*The amount of mutant PRPF31 mRNA is strongly reduced with respect to wild-type transcripts*. We measured the expression of mutant *PRPF31* alleles relative to their wild-type counterparts in lymphoblastoid cell lines derived from 9 heterozygous patients carrying 1 of these 6 mutations: c.177+1delG, c.323-2A>G, c.877_910del, c.319C>G, c.856-2A>G and c.1115_1125del. After cDNA synthesis, the region encompassing the mutation was amplified by semiquantitative RT-PCR using specific primers that could amplify both alleles in the same reaction. Relative quantification of the produced PCR fragments, performed using 2 independent techniques, gave the same results overall and was in agreement with our previous results (28). We found that, for all cell lines analyzed, the amount of mRNA containing the mutation was markedly reduced in comparison with transcripts derived from the *PRPF31* wild-type allele (Figure 2). Depending on the cell line analyzed, the expression of mutant mRNA alleles was reduced to between 6% and 25% (average = 14%) of the nonmutant *PRPF31* transcript. For cell lines with the c.1115_1125del mutation, low levels of both predicted mutant mRNA forms were detected: the long form (carrying a canonical splicing pattern and the 11-bp deletion, hypothesized to be NMD-insensitive) and the short form (carrying the exon 10–exon 12 rearrangement, predicted to be potentially subject to NMD). To exclude the possibility that the observed phenomenon could be related to lymphocyte immortalization, we also measured allelic *PRPF31* mRNA expression in leukocytes extracted from total blood of 4 of these 9 patients (14266, 12688, 13190, and 14284) and found a similar reduction in the mutant allele of between 6% and 30% (data not shown).

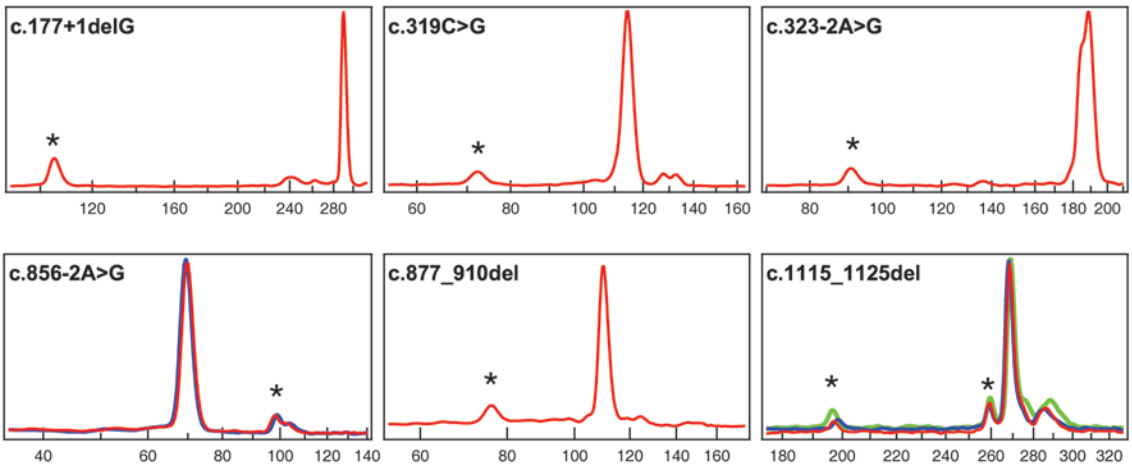


**Figure 2**
Capillary electrophoresis of semiquantitative RT-PCRs spanning 6 different *PRPF31* mutations. We analyzed unprocessed PCR products obtained with 6 different primer pairs, specific for each mutation, that could simultaneously amplify the wild-type and the mutant mRNA (cDNA) in the same reaction. The single curves shown are representative of 5 replicates from each of 3 independent cultures. The *x* axis indicates the approximate size (in bp) of the DNA fragments, whereas the *y* axis shows the amount of PCR product normalized to the peak height of the wild-type allele. PCR products originating from the mutant alleles are indicated by asterisks. For c.1115_1125del, the peak at ~197 bp is the short form produced by the skipping of exon 11, whereas the peak at ~260 bp is the NMD-insensitive long-form mRNA allele containing the 11-bp deletion. For the c.856-2A>G mutation, the red curve corresponds to cell line 12688, whereas the blue curve corresponds to cell line 13190. For the c.1115_1125del mutation, the PCR products from cell lines AG0293, AG0305, and AG0307 are indicated by the green, red, and blue curves, respectively.

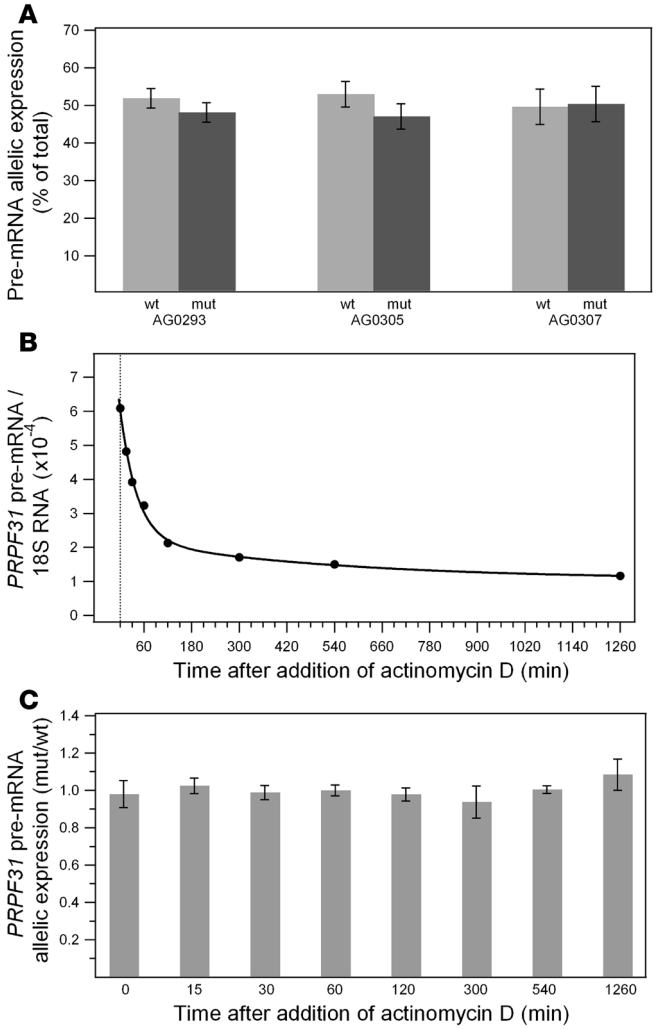


**Figure 3**
Allelic expression of nuclear *PRPF31* pre-mRNA in c.1115_1125del heterozygotes. (**A**) The mutant and wild-type alleles in cell lines from 3 patients at steady state were expressed at a ratio of approximately 50:50. (**B**) When cell line AG0307 was treated with actinomycin D to block RNA transcription, the amount of *PRPF31* pre-mRNA was progressively depleted because of splicing (0–60 minutes) followed by its intrinsic decay (after 60 minutes; data on specific effects of splicing and decay are not shown). (**C**) Nonetheless, the ratio between wild-type and mutant nuclear pre-mRNA was approximately the same and remained constant over time, which indicated that the half-lives of the 2 forms are the same.

*Mutant pre-mRNA molecules are not transcribed at a reduced rate and have an intrinsic stability comparable with that of normal transcripts*. To assess whether the observed low amounts of mutant mRNA molecules were due to an allele-specific reduction in their transcription rate (e.g., because of a weaker promoter), or to their intrinsic stability, we measured the amounts of nuclear pre-mRNA for both mutant and wild-type alleles. We selected the c.1115_1125del change as a model for all *PRPF31* mutations, because this mutation was most prevalent in our patient cell lines. Allele-specific real-time PCR in cell lines at steady state from 3 different patients carrying this mutation showed that the amount of nuclear pre-mRNA was approximately the same for both the wild-type and mutant alleles (Figure 3A).

Subsequently, we selected one of these cell lines (AG0307) and measured the amount of *PRPF31* transcripts in nuclear pre-mRNA over a 21-hour time course, after blocking the synthesis of new RNA molecules by incubating the cells with the inhibitor of transcription actinomycin D. We performed *PRPF31* non-allele–specific real-time PCR, normalized to individual PCR efficiencies, versus the amount of 18S rRNA. The results showed that although the amount of *PRPF31* pre-mRNA decreased after blocking transcription (Figure 3B), the relative proportion of the mutant to nonmutant allele transcripts, as measured by semiquantitative RT-PCR, remained unchanged (Figure 3C). This indicated that the nuclear pre-mRNA molecules carrying the mutation had a half-life similar to that of their wild-type counterparts.

Taken together, these results indicate that mutant and wild-type *PRPF31* alleles are transcribed at approximately the same rate and also have a comparable intrinsic stability. Therefore, at least for this particular DNA change, the presence of the mutant allele does not appear to interfere with either its own transcription or the amount of pre-mRNA to be processed by splicing.

*Carriers of PRPF31 mutations have reduced amounts of PRPF31 protein and do not express detectable amounts of mutant protein*. To assess to what extent the observed reduction in *PRPF31* mRNA levels translated into cellular PRPF31 protein abundance, total protein extracts were prepared from all lymphoblastoid cell lines carrying *PRPF31* mutations and from 4 control cell lines. PRPF31 protein abundance was quantified via Western blotting using a specific N-terminal PRPF31 antibody and analyzed with the Odyssey Infra-Red Detector (LI-COR Biosciences). This system uses a 2-color infrared detector that, unlike standard autoradiography film, allows the detection and quantification of fluorescent bands with a sensitivity of 1.2 pg across a 4,000-fold linear range.

For each cell line, we performed 4 replicate gels to simultaneously detect and quantify the abundance of PRPF31 (Figure 4A, green bands) and β-actin (Figure 4A, red bands). We consistently observed a decrease in the abundance of full-length PRPF31 with respect to normal controls (Figure 4, A and C). When combined, the PRPF31 content of cell lines derived from patients with RP was on average 69% of that derived from controls. This reduction was statistically significant ($P = 0.0006$, 2-tailed Student's $t$ test). The results were identical when the PRPF31 abundance was normalized relative to the abundance of β-actin (as shown) or relative to the average PRPF31 abundance across the whole gel (data not shown). Similar results were observed for multiple protein extractions and replicate gels (data not shown).

Unlike in previous studies, the antibody generated in this study has the ability to detect truncated PRPF31 protein products, because it was generated against the N terminus. However, we were unable to detect the presence of any truncated proteins of the sizes predicted to be produced by the mutant alleles (Figure 4A, boxed for each mutation). The sensitivity of our experimental setup was empirically determined using serial dilutions of total protein extracts and was shown to be able to detect PRPF31 proteins with a relative abundance of 3%–4% with respect to the observed full-length PRPF31 protein (data not shown).

Cell lines with the c.1115_1125del mutation were predicted in silico to produce an NMD-insensitive mRNA transcript (the long form), which can result in a truncated protein of 469 amino acid

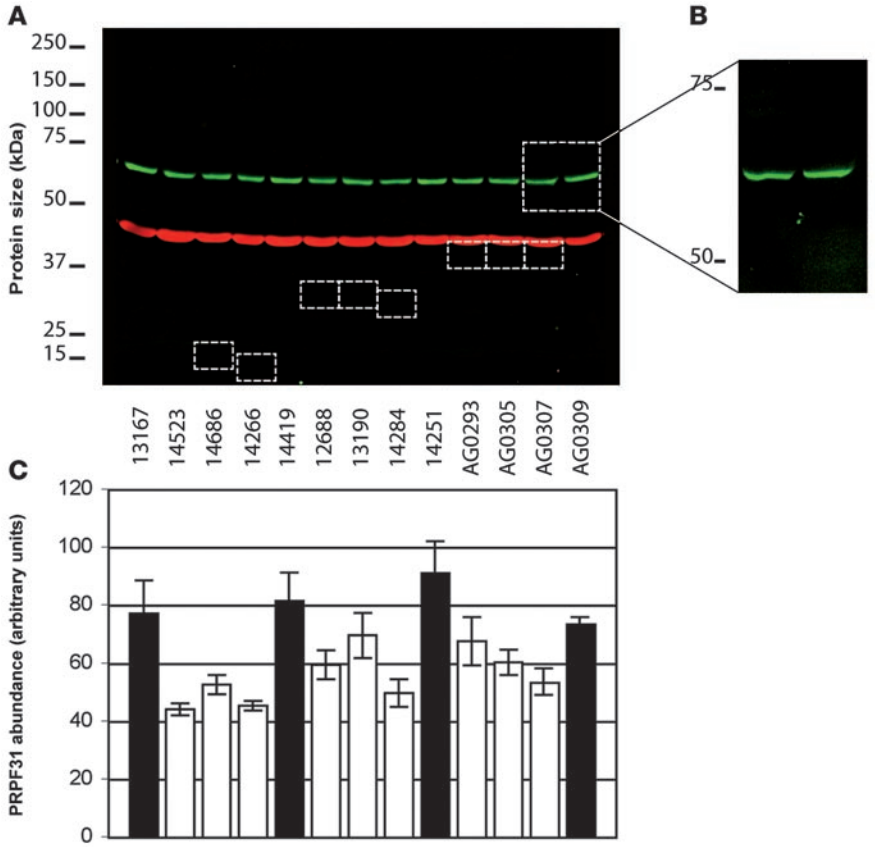


**Figure 4**
Differential protein abundance and absence of truncated PRPF31 proteins in cell lines derived from patients. (**A**) Quantitative SDS-PAGE (10%) of total protein extracts from various patient cell lines and controls. Simultaneous infrared detection of proteins was achieved with a highly specific N-terminal anti-PRPF31 antibody (green) and a β-actin control (red). The white dotted boxes indicate the expected position of mutant proteins derived from NMD-sensitive alleles, if they were present. Protein size cannot be predicted from the mutation in cell line 14523; however, it is likely to lack the N-terminal epitope for detection with this antibody. (**B**) Original magnification of another quantitative, high-resolution SDS-PAGE (15%) using protein extracts from a cell line carrying the c.1115_1125del mutation (AG0307) and from an unaffected control (AG0309). A high-percentage acrylamide gel, run over a longer time, was used to resolve the small size difference between PRPF31 proteins derived from the wild-type and the mutant long-form mRNA. However, only the full-length (wild-type) PRPF31 form was visible. (**C**) Quantification of PRPF31 protein abundance from cell lines derived from patients using a combination of 4 independent gels, including the one depicted in **A**, and normalized to the abundance of β-actin. Black bars, control cell lines; white bars, cell lines from patients with *PRPF31* mutations.

residues (vs. 499 aa of full-length PRPF31), containing a unique sequence of 98 C-terminal amino acids. To specifically detect this 3- to 4-kDa smaller PRPF31 mutant form, we performed high-resolution Western blotting with the same antibody (15% PAGE gels, run for 120 minutes,) and analyzed them with the same fluorescent quantitative system. Despite the predictions and the fact that the long mRNA form is indeed insensitive to NMD (see below), no mutant protein corresponding to the long mRNA form was detected (Figure 4B). This observation was similar to that for all other PRPF31 mutations examined.

*Full-length PRPF31 protein is not mislocalized in patient cells.* A C-terminal anti-PRPF31 antibody was used to colocalize full-length PRPF31 protein in patient-derived cell lines via indirect immunofluorescence. Consistent with observations in HeLa cells (32), PRPF31 staining in our set of lymphoblastoid cell lines was restricted to a punctate subset of nuclear structures without staining the nucleoli or cytoplasm (Figure 5). Staining with the splicing speckle marker SC35 (Figure 5), which identifies the portions of the nucleus rich in splicing snRNPs and other splicing proteins, showed that these compartments were strongly but not completely colocalized (Figure 5, merged channels).

Importantly, full-length PRPF31 remained in these nuclear compartments in cell lines from patients with RP, and the distribution pattern of PRPF31 and SC35 was indistinguishable from that displayed by unaffected controls. Previous data has shown that 95% depletion of PRPF31 protein by RNAi results in the accumulation of spliceosome components elsewhere in the nucleus (33). Our data indicate that full-length PRPF31 protein from patient-derived cell lines, although less abundant, is not sequestered in other subnuclear compartments and suggest that the protein is present and likely to be functioning normally.

*Degradation of mutant alleles is a consequence of an active process: NMD.* All mutations analyzed are potentially susceptible to degradation at the mRNA level by NMD, because they are predicted to result in the creation of PTCs before the last exon, either directly or indirectly (28, 30). To test whether NMD was responsible for the observed reduction in mRNA abundance for all our mutant transcripts, we treated each cell line with cycloheximide and emetine — 2 potent inhibitors of NMD. Both drugs increased the level of mutant mRNA in all patient cells except for cell line 14523, in which the c.177+1delG mutation causes the skipping of exon 2 (Figure 6). These data indicate that NMD plays an active role in the degradation of *PRPF31* mutant mRNA alleles that contain a PTC. Quantification of the relative expression of mutant mRNA versus wild-type mRNA by semiquantitative RT-PCR showed that this ratio increased 3 to 9 times, depending on the mutation, when cells from patients were grown in the presence of cycloheximide or emetine. In agreement with previous data obtained with different genes and mutations, treatment with these NMD inhibitors was unable to fully restore the expression of the mutant mRNA alleles, and emetine had a stronger inhibitory effect than did cycloheximide (34, 35).

For patients bearing the c.1115_1125del mutation, inhibition of NMD only increased the amount of transcripts carrying the skipping of exon 11 (short form), whereas this treatment seemed to have little or no effect on the long form carrying the 11-bp deletion (Figure 6). To verify whether the long form of the c.1115_1125del mRNA was indeed refractory to NMD and could potentially be

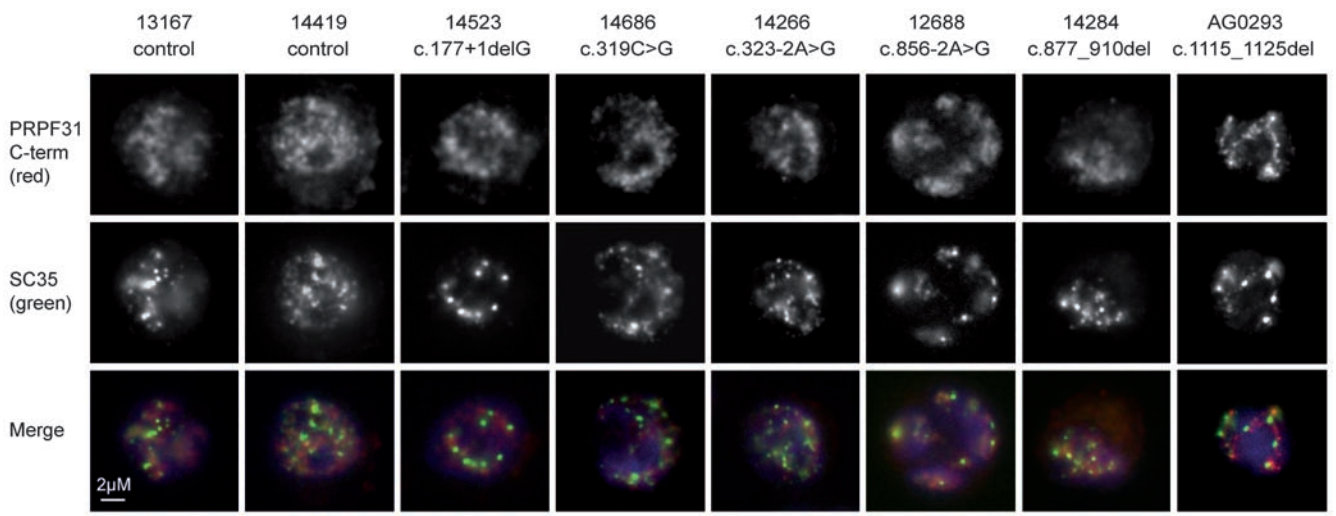


**Figure 5**
Full-length PRPF31 protein is not mislocalized in patient-derived cell lines. Full-length PRPF31 (red) was detected by indirect immunofluorescence using a C-terminal antibody. A speckled staining pattern that was exclusively nuclear was observed, similar to PRPF31 localization in other cell types. Merged images demonstrated extensive, but not complete, colocalization with the marker for splicing speckles SC35 (green). No differences in staining patterns could be observed between affected individuals and unaffected controls, which indirectly suggests that PRPF31 function may not be impaired in patients. Blue indicates DAPI nuclear staining, and the scale bar applies to all images.

translated into truncated PRPF31 proteins, we treated all cell lines carrying the c.1115_1125del mutation with 3 NMD inhibitors (cycloheximide, emetine, or puromycin) and specifically measured the expression of the long mutant mRNA form versus the *PRPF31* wild-type allele in both nuclear and cytoplasmic mRNA extracts by allele-specific real-time PCR. As a control, we repeated the same procedures on cell line 14266, which bears a mutation that is clearly susceptible to NMD. Our results showed that, irrespective of the NMD inhibitor used, the amount of *PRPF31* mRNA long mutant form was never rescued (Figure 7), neither for cytoplasmic nor nuclear RNA. These data indicate that the long form of this mutation escapes NMD and should therefore potentially be available for translation into a truncated protein. Yet, our experiments failed to detect this truncated protein. Taken together, these observations potentially implicate the presence of protein degradation pathways in the suppression of this deleterious PRPF31 allele.

*Inhibition of UPF1 and simultaneous block of lysosomal trafficking and proteasome activity does not rescue mutant PRPF31 proteins*. Our data indicate that there is a substantial discrepancy between the presence of mutant mRNA escaping NMD (14% of wild-type *PRPF31* mRNA, on average, Supplemental Table 1; supplemental material available online with this article; doi:10.1172/JCI34211DS1) and the lack of protein resulting from these mRNAs. Although many hypotheses can be made, one possible explanation for this discrepancy could be that mutant PRPF31 proteins fail to fold properly and/or are quickly degraded by housekeeping cellular mechanisms. To test this assumption, we investigated whether mutant PRPF31 proteins accumulated after stabilization of their respective mRNAs, along with inhibitors of protein degradation pathways.

Because NMD inhibitors such as cycloheximide, emetine, and puromycin block translation, we attempted to selectively silence the essential NMD gene *UPF1* by RNAi using synthetic double-strand RNA (36), pSUPER-derived constructs (37), and lentiviral infection (38). Although gene-silencing experiments were successful in standard laboratory cell lines (HeLa) and despite the high transfection/infection efficiency, lymphoblastoid cell lines derived from patients never exhibited any *UPF1* downregulation (data not shown) — a difficulty also observed by others under similar conditions (39). Therefore, we adopted a protocol using wortmannin to block phosphorylation and, thus, the activation of the essential NMD protein UPF1 without inhibiting protein synthesis (40). Except for the NMD-insensitive cell line 14523, wortmannin treatment resulted in a substantial rescue of mutant mRNA, as measured by semiquantitative RT-PCR, that in some cases approached the level of the nonmutant allele and on average reached a level of 47% of the wild-type allele (Figure 8A, Supplemental Table 1). Treatment with wortmannin in conjunction with the lysosome inhibitor chloroquine and the proteasome inhibitor MG132 showed similar results and, in some instances, even increased the expression of the mutant allele above that of the wild-type allele. Despite this substantial increase in mRNA level, none of the treatments resulted in the appearance of any truncated PRPF31 polypeptides (Figure 8B), which indicated that the reduced stability of PRPF31 proteins resulting from stabilized mRNA alleles, if they exist at all, is likely independent of the proteasomal and lysosomal proteases. These data are consistent with our previous observation that the long mutant c.1115_1125del mRNA allele failed to result in a detectable protein product, even though it was not subject to NMD.

## Discussion

The vast majority of *PRPF31* mutations that cause RP result in the creation of termination codons before the natural stop of the reading frame. In the present study, we investigated 6 different *PRPF31* mutations that recapitulate this common situation using lymphoblastoid cell lines derived from 9 patients with autosomal dominant RP. Initially we demonstrated that there is a striking difference in mRNA expression levels between mutant and nonmutant alleles. We then showed that this difference could not be attributed to a modification in transcriptional activity of the mutant allele or to instability of the mutant mRNA transcript. We further demon-

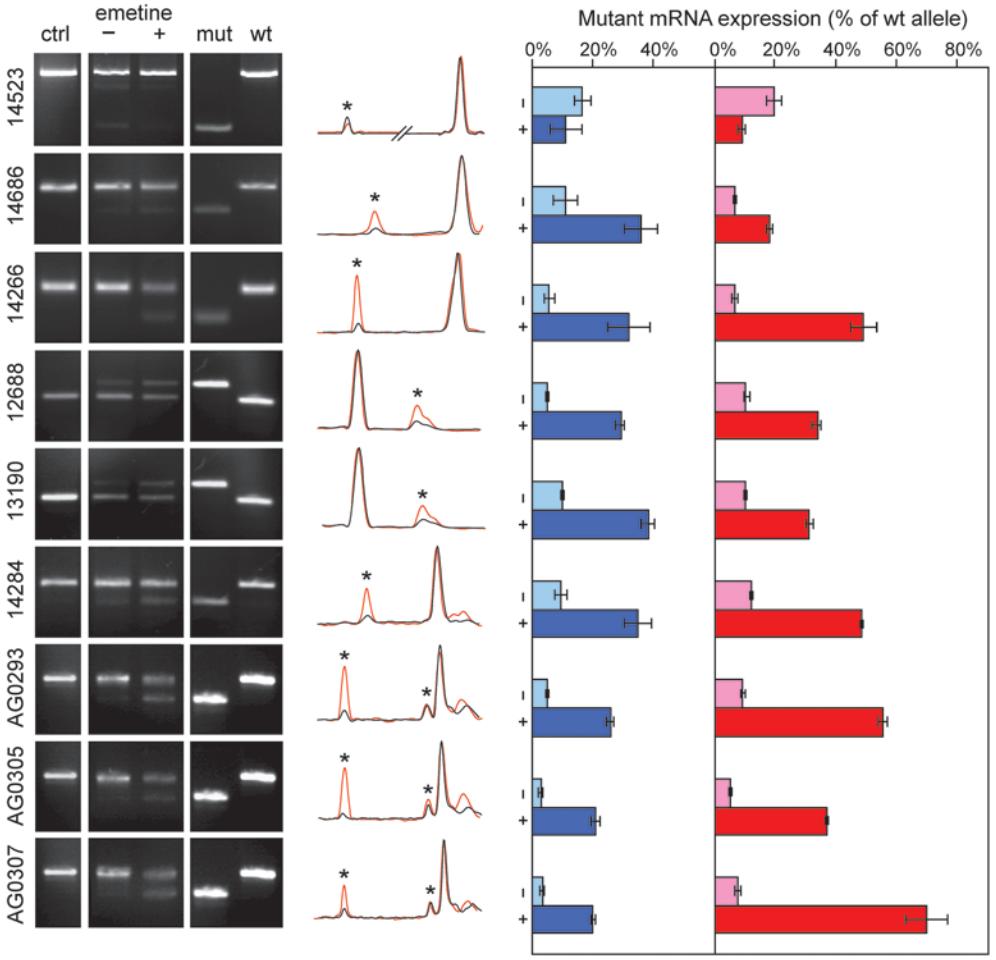


**Figure 6**
Quantitative rescue of NMD-sensitive mutant mRNA alleles with cycloheximide and emetine treatment. Representative images of agarose gel and capillary electrophoresis of semiquantitative RT-PCR products from mutant *PRPF31* transcripts are shown (for emetine only). For each cell line, PCR products were always run on the same agarose gel, but they were not contiguous. Data shown summarize measurements of 5 PCR replicates from 3 (emetine) or 4 (cycloheximide) treatments on independent cultures for each cell line. Cell line identification codes are shown on the left. The term *ctrl* refers to semiquantitative RT-PCR from a control cell line (GM104848). Throughout, the symbols + and – indicate the presence or absence of NMD inhibitors in the cell culture medium. The terms *mut* and *wt* correspond to PCR products from plasmids containing the mutant and wild-type alleles, respectively. Electrophoretograms were normalized to the height of the wild-type peak and aligned automatically. Black and red curves indicate the absence or the presence of emetine in the culture medium, respectively, and asterisks highlight PCR products derived from the mutant mRNA form. Treatment with either cycloheximide (blue bars) or emetine (red bars) partly restored the expression of NMD-sensitive mutant alleles and had no effect on NMD-insensitive mutant alleles. For cell lines AG0293, AG0305, and AG0307, bars show only the change in the NMD-sensitive allele (short form). Data presented as bar graphs are the combination of both densitometry values of agarose gel bands (ImageJ software) and the integration of peak from capillary electrophoresis (Biocalculator software).

strated that all mutations resulting in PTCs located before the last exon result in mRNA alleles that are actively degraded by NMD. Of the small proportion of mutant transcripts that are still detectable, all fail to be translated into proteins, at least to a level detectable by highly sensitive and quantitative immunoblotting. Patient cell lines were also shown to contain a decreased level of full-length PRPF31 protein, the subnuclear localization of which cannot be distinguished from that of controls and is perhaps indicative of its normal functioning. Altogether, these data indicate that NMD plays a central role in the degradation of the mutant mRNA containing PTCs, which protects cells from potentially negative effects of these transcripts and their encoded products. Furthermore, we concluded that all of the *PRPF31* mutations analyzed result in null alleles and that heterozygous patients who carry them can be considered functional hemizygotes.

We investigated dominant mutations in *PRPF31*, a pre-mRNA splicing factor that is essential for cell survival, yet causes a tissue-specific phenotype such as nonsyndromic retinal degeneration. We adopted this system as an extreme example of the elevated genetic and allelic heterogeneity displayed by RP, for which a similar phenotype may correspond to a high number of mutations encoded by many different genes (5). For this kind of investigation and for medical research in general, access to suitable material for molecular and functional studies of diseases is of paramount importance. The ex vivo cell cultures used in this study naturally express *PRPF31* and represent, we believe, the best possible experimental model for

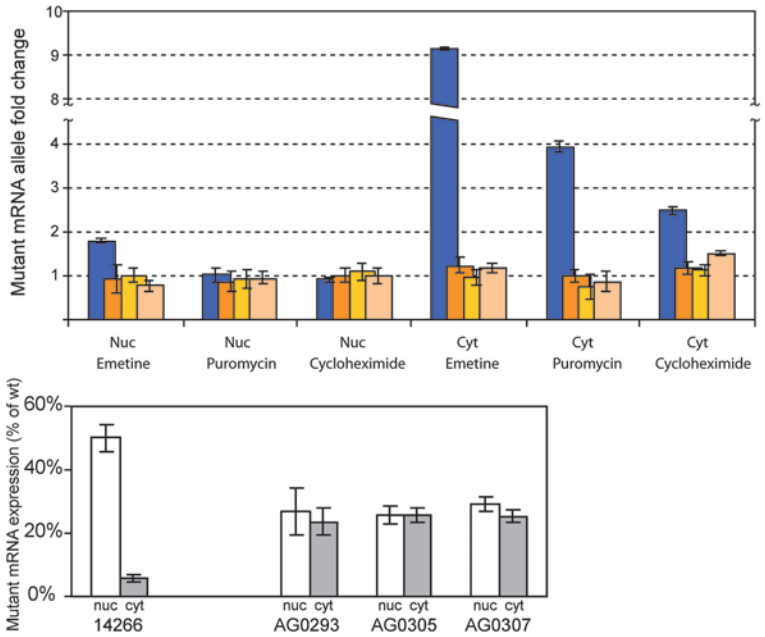


**Figure 7**
The mRNA containing the c.1115_1125del mutation (long form) is insensitive to NMD. Treatment with emetine, puromycin, or cycloheximide partly rescued the relative abundance of mutant mRNA in the cell line 14266 (positive control, blue bars), but not the mRNA containing the 11-bp mutation in exon 11 (long form) extracted from cell lines AG0293, AG0305, AG0307 (respectively from left to right, bars in shades of orange), as measured by allele-specific real-time PCR. Nuclear (Nuc) and cytoplasmic (Cyt) mutant mRNA fold changes for each cell line (long form only) were calculated by dividing the mutant/wild-type allelic ratio following each NMD inhibitor treatment by the corresponding mutant/wild-type allelic ratio with no drug treatment. The rescue of the 14266 mutant mRNA was more pronounced in the presence of emetine and was more effective on Cyt RNA. Below: Allele-specific real-time PCR measurement of the long mRNA form in untreated cells showed that NMD did not affect the mRNA level of the long form of the c1115_1125del mutant allele, but was active on the 14266 mutant mRNA. Data represent the average of 3 real-time PCR replicates for each cell line and each treatment.

studying *PRPF31* molecular genetics, because retinal biopsies are obviously not practicable, transgenic animals with similar splicing factor mutations have thus far failed to show any phenotype (41–44), and cell-based transfections of mutant protein constructs do not recapitulate the natural situation of a partial lack of PRPF31.

Quantification of *PRPF31* mRNA extracted from whole cells from all patient-derived cell lines showed a significant underrepresentation of mRNA molecules originating from the mutant DNA allele, in agreement with previous results based on the measurement of allelic or total transcripts (28, 30, 45). The magnitude of this decrease showed some variation and was possibly mutation-dependent; however, the reduction was consistent in all cells analyzed (Figure 2). Total mRNA at steady state is influenced by a number of processes, including the rate of transcription and the stability of transcripts. By quantifying allelic expression levels of pre-mRNA in the nucleus, we excluded the possibility that mutant *PRPF31* RNA is transcribed at a reduced rate (Figure 3A) or has a reduced intrinsic stability as compared with nonmutant transcripts (Figure 3, B and C). We therefore conclude that posttranscriptional mechanisms are central to the observed cellular phenotype.

Despite in silico predictions, mutant *PRPF31* mRNA degradation by NMD has never been proven. Inhibiting NMD with chemical treatments results in an increase of all *PRPF31* mRNA alleles that encode PTCs located before the last exon, which indicates that this cellular mechanism is indeed responsible for their active degradation and for the overall reduction in *PRPF31* expression (Figure 6). An exception to this trend is seen with the mutation c.177+1delG, which also displays reduced amounts of mutant transcripts but seems to be insensitive to NMD inhibition. This mutation is peculiar, because it causes the skipping of exon 2, which contains the natural start codon of the reading frame (28), and results in the likely use of an alternative AUG. Multiple out-of-frame AUG codons exist in the *PRPF31* sequence, which potentially leads to PTC-containing, NMD-sensitive mRNA transcripts. However, in silico analysis of possible *PRPF31* AUG codons matching the features of natural start sites (46) indicated that all 14 potential translation start sites are in-frame with the *PRPF31* natural stop codon, the first 3 of which lie within exon 2. It has been shown that the loss of multiple in-frame AUG codons at the beginning of the coding sequence results in a substantial decrease in mRNA expression (47). Therefore, the reduced expression level of this NMD-insensitive mutation could be explained by this phenomenon. Furthermore, we excluded, on the basis of real-time PCR experiments using primers that are located outside the rearrangement (28), the possibility that the c.177+1delG change could result in a leaky mutation, producing only occasionally the skipping of exon 2 but overall resulting in a regular amount of spliced mRNA. Although we do not have enough data to support a definitive genotype-phenotype correlation, it is of clinical interest that an individual who carries this mutation exhibits a milder phenotype by ERG than do individuals with other mutations (Table 2).

The mutation c.1115_1125del removes an exonic splicing enhancer in exon 11 and produces 2 distinct mRNA forms. A long form that displays a regular splicing pattern, carries this 11-bp deletion, and is NMD-insensitive, and a short form that exhibits an exon 10–exon 12 splicing rearrangement creates an NMD-sensitive PTC (Figure 1) (30). A comparison of our results for pre-mRNA with those for steady state RNA measurements indicated that *PRPF31* DNA alleles with the c.1115_1125del are mostly spliced into the short, NMD-sensitive RNA form (~86%), whereas the long, NMD-insensitive mRNA represents the remaining ~14% of the mutant allele (Figure 3, Supplemental Table 1). The reduction in expression of the long mRNA mutant form is thus due to a preferential bias in favor of the short form during splicing, rather than to degradation via the NMD pathway. Indeed, the long form is untouched by the NMD process, remains constant in nuclear and cytoplasmic extracts (Figure 7), and is potentially available as a template for protein synthesis. It is of interest to note that, although within the same range, the values relative to the percentage of the mutant long mRNA form with respect to the wild-type mRNA are slightly different when measured from total RNA and by semiquantitative RT-PCR (~14%; Supplemental Table 1) and when quantified after cellular fractionation by

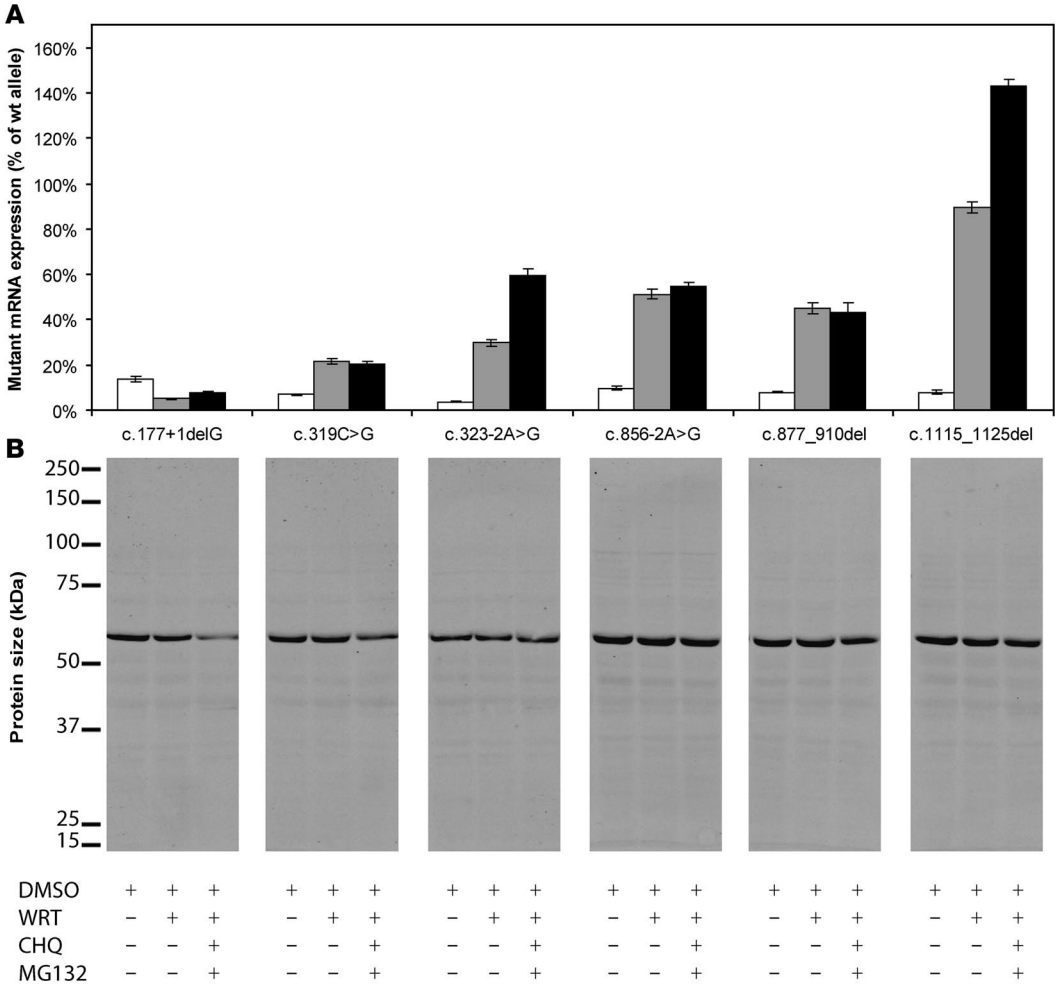


**Figure 8**

Inhibition of NMD and the lysosomal and proteasomal protein degradation pathways does not rescue the synthesis of mutant PRPF31 proteins. (**A**) The addition of wortmannin (WRT) markedly enhanced the stability of most mutant forms of mRNA as measured by semiquantitative RT-PCR, except for mRNA derived from the c.177+1delG mutation that skips the initiation codon. A similar and sometimes more pronounced rescue was observed in the presence of WRT along with the lysosome inhibitor chloroquine (CHQ) and the proteasome inhibitor MG132. Data summarize measurements of 5 PCR replicates from 3 independent cultures treated as shown for each of the 6 cell lines. (**B**) Quantitative SDS-PAGE of the corresponding protein extracts from the same cell preparations. WRT treatment alone did not rescue the expression of any mutant proteins, nor did the addition of lysosomal and proteasomal inhibitors. Sample 14523 can be used as a negative control because it lacks the N-terminal epitope needed for recognition with this antibody.

allele-specific real-time PCR (~25%; Figure 7). Although we have no proven explanation for this discrepancy, it is likely that the different methods used may have been responsible.

To study the subsequent effect of *PRPF31* mutations at the protein level, we developed an anti-PRPF31 antibody specific to the first 15 N-terminal amino acids. This antibody is potentially able to recognize all PTC-containing mutations (except for c.177+1delG), in contrast with all currently available antibodies that recognize only C-terminal epitopes. Quantitative Western blotting showed that the decrease in total *PRPF31* mRNA expression was reflected in the reduced abundance of PRPF31 protein in lymphoblastoid cell lines from all patients with *PRPF31* mutations, mostly as a direct consequence of NMD targeting of mutant transcripts. However, whereas all are heterozygotes, these cell lines appeared to produce more than 50% of PRPF31 full-length protein (~69% on average; Figure 4), with respect to controls. A similar tendency was previously observed at the mRNA level, as measured by real-time PCR and microarray hybridization, in a comparison of patients with *PRPF31* mutations and healthy controls (28). These values are potentially explained by a feedback compensatory mechanism that could be triggered by the lack of functional PRPF31, a mechanism worthy of further investigation.

Interestingly, although we were able to detect quantitative differences in full-length PRPF31 in these Western blots, we were unable to detect any truncated PRPF31 proteins resulting from the translation of any mutant alleles (Figure 4). This finding is significant because we demonstrated that this detection system was sensitive enough to identify PRPF31 variants as rare as 3%–4% of the full-length form and that the amount of mutant *PRPF31* mRNA that escapes degradation was on average 14% of that of the wild-type transcripts. These transcripts may represent mRNA that has been marked for NMD and not yet degraded or mRNA that is not effec-

tively translated. Alternatively, the truncated proteins derived from this mRNA could be quickly degraded or intrinsically unstable. Indeed, there are a number of examples in patient-derived cell-based systems where protein products from mutant alleles cannot be detected and are suggested to be unstable (48–53). Meanwhile, the detection of truncated proteins after inhibition of NMD remains atypical (39, 54). The discrepancy between the presence of mutant transcripts and the complete lack of mutant proteins is particularly relevant for the long mRNA form originating from the c.1115_1125del mutation, which amounts to 14% of the wild-type mRNA, is not targeted for NMD, and nonetheless does not seem to result in any truncated protein. Altogether, these data suggest the presence of an additional control mechanism that prevents the formation of truncated proteins, possibly one that is connected to NMD and/or to the splicing process.

We addressed this concept by treating cell lines containing *PRPF31* mutations with wortmannin, which inhibits NMD while preserving protein synthesis, and observed a strong increase in the production of mutant mRNA. However, most interestingly, there was no complementary detection of truncated proteins, even at mRNA levels that were equal to those of the wild-type allele (Figure 8). Similar observations have been reported for one specific example, where expression of 20 *BRCA1* mutant alleles and 1 *CHK2* mutant allele was elevated in the presence of wortmannin (39). When treated in conjunction with the lysosome inhibitor chloroquine, 2 truncated BRCA1 proteins were detected, which suggests that these mutant proteins were unstable and rapidly degraded; however, no such truncated bands were detected for any of the other mutations tested. Using a similar approach, we supplemented the culture medium of all our cell lines with wortmannin, chloroquine, and the proteasome inhibitor MG132. Despite this treatment, we could not rescue the expression of any mutant PRPF31 protein forms, which suggests that lysosomal and proteasomal degradation pathways have little or no impact on the abundance of PRPF31 truncated proteins in vivo and that, perhaps, the mRNA encoding these mutations is not translated.

There is strong support for a lack of translation of similar mutant alleles in cancer cell lines by a process known as nonsense-mediated translational repression (NMTR). In a recent study, a number of natural mutations that encode PTCs before the last exon were shown to escape NMD, yet truncated protein transcripts were not detected and their mRNAs were not associated with polysomes (55), which indicates that the mutant mRNA is not translated. In light of this finding, we suggest that the small amount of mRNA transcripts present in our patient cell lines is likely subject to NMTR, which prevented the synthesis of truncated proteins. Likewise, mutant mRNA that is present at elevated levels, due to the inhibition of NMD, is perhaps also a target for NMTR and hence not translated. Therefore, products of mutant alleles containing PTCs would appear to be degraded or inactivated by 2 complementary mechanisms, NMD and NMTR, which effectively prevent the synthesis and remove all traces of truncated proteins resulting from their transcription and translation.

To date, some *PRPF31* mutations have undergone functional analysis. For the p.Ala194Glu and p.Ala216Pro missense changes, ectopic expression of mutant cDNA in standard laboratory cell lines or by in vitro assays demonstrated that these 2 amino acids are essential for the interaction with the spliceosome protein 15.5K and U4 snRNA (56, 57). Furthermore, plasmids carrying these mutations produce PRPF31 proteins that are unable to translocate into the nucleus with high efficiency and, therefore, have a reduced function in the splicing process (56). Although these important data shed new light on the functional role of PRPF31 in pre-mRNA splicing, they do not represent the situation commonly found in patients with *PRPF31*-linked RP, whereby a majority of the mutations result in PTCs. Other experiments in transfected cells have tested the effect of the expression of 2 truncated forms of the PRPF31 protein, theoretically derived form the c.769_770insA and c.1115_1125del mutations (58, 59). Unfortunately, these experiments have little to no biological or clinical relevance, considering our main findings on the lack of expression of c.1115_1125del alleles and other PTC-containing alleles under normal conditions and that both cDNA constructs used were incorrectly truncated at the site where the frameshift occurs and not at the site of the PTC. Significant and very interesting data exist on the effects of RNAi-based *PRPF31* inactivation, which mimic more closely the situation demonstrated by findings and in patients with large deletions. These experiments showed that a strong PRPF31 depletion leads to the accumulation of essential spliceosome components in Cajal bodies and, therefore, likely to the block of the splicing process (33). PRPF31 immunodepletion experiments in mammalian cells induced a block in the formation of the catalytic tri-snRNP particles (32), and complete loss of PRPF31 has also been shown to be lethal in yeast (7). Our data show that there is an underrepresentation, but not a complete absence, of PRPF31 protein in patient cell lines and that the non-mutant protein is localized normally within these cells. This finding further supports the notion that the PRPF31 protein present in patients functions normally, although this cannot be directly tested, and thus the situation in patients is very different from that observed in knockdown and immunodepletion experiments.

Taken together, our results are particularly important concerning the molecular etiology of RP, because they indicate that PRPF31 mutations very likely cause RP via a haploinsufficiency mechanism rather than through a dominant-negative effect. We cannot completely exclude the presence of small, undetectable amounts of truncated forms of PRPF31 or of tissue-specific NMD (60, 61) that are potentially active in lymphoblastoid cell lines but not in the retina. However, both of these possibilities are unlikely given that recent genetic screenings have shown that a non-negligible portion of patients are true hemizygotes who carry large deletions in the *PRPF31* region (24, 25). The crucial question that remains is how is it possible that PRPF31, an essential component of the spliceosome (a macromolecular machinery that is vital in all eukaryotic organisms) and a protein necessary for cell survival, is implicated in a tissue-specific, non-life-threatening phenotype such as dominant RP. Some hypotheses implicate the alteration of alternative splicing in the retina or of retinal-specific genes; others assume an effect on nearly all photoreceptor transcripts, a cell type in which demand for mRNA and therefore splicing is perhaps elevated. Other explanations take into account a possible alternative "moonlighting" function, unrelated to splicing, which PRPF31 performs specifically in the retina. Whatever the mechanism, what is certain is that a mild reduction in the PRPF31 content somehow results in certain retinal-specific deficiencies. Finally, our finding that haploinsufficiency is the likely mechanism for nearly 90% of all known *PRPF31* mutations has important consequences for future gene therapy in an easily accessible tissue, where supplementary expression of a common full-length *PRPF31* cDNA construct could be the treatment for many genetically different cases.

## Methods

*Patients*. Patients 12688 to 14686 were seen for a complete eye examination, which included kinetic visual fields and full-field ERGs obtained with computer averaging and narrow bandpass filtering, as described previously (2). Visual fields measured with a Goldmann perimeter were quantified with respect to total remaining visual field areas. ERGs were obtained after 45 minutes of dark adaptation and were quantified with respect to peak-to-peak amplitudes. Biological samples were donated by the patients after they provided informed consent in accord with the Declaration of Helsinki. Patients AG0293, AG0305, and AG0307 were described previously (31).

*Cell culture and drug treatment*. The Epstein-Barr virus immortalized lymphoblastoid cell lines used in this study were derived from affected patients (Table 1) and unaffected controls (patients 13167, 14419, and 14251) and cultured as previously described (28). Cell lines from a family segregating the c.1115_1125del mutation (10, 31, 62) (Table 1) and a control (AG0309) were purchased from the European Collection of Cell Cultures. Another normal control cell line (GM104848) was purchased from the Coriell Cell Repository.

Treatment with cycloheximide (Sigma-Aldrich) was performed by incubating 10 million cells for 4 hours in the presence of medium supplemented with 28 μg/ml of this chemical (from a 100 mg/ml master solution prepared in DMSO), according to published protocols (63). Similarly, treatments with emetine and puromycin were carried out by incubating 10 million cells with 300 μg/ml of these drugs (Sigma-Aldrich) for 6 hours. Inhibition of NMD through the inactivation of UPF1 phosphorylation, blocking of lysosomal trafficking, and inactivation of the proteasome were achieved by treating 5 million cells with 100 μM wortmannin, 100 μM chloroquine, or 50 μM MG132, respectively, for 6 hours. All negative controls were treated with a relevant volume of DMSO alone.

Transcription inhibition experiments were performed by growing 100 million lymphoblastoid cells in the presence of 5 μg/ml of actinomycin D (Sigma-Aldrich). Aliquots of 10 million cells were taken at different time points (0, 15, 30, 60, 120, 300, 540, and 1260 minutes) after the addition of actinomycin D.

*RNA extraction and cDNA synthesis*. For total RNA extraction, cells were homogenized with QIAshredder columns (QIAGEN), and RNA was isolated using the RNeasy Kit (QIAGEN) according to the manufacturer's instructions and including on-column DNAse treatment. Total RNA was used as a retrotranscription template to generate all semiquantitative and real-time PCR data presented in this work. An exception to this method involved the analysis of the effects of NMD inhibitors on nuclear and cytoplasmic mRNA, performed on the long *PRPF31* mRNA form from cell lines AG0293, AG0305, and AG0307 and on the mutant *PRPF31* mRNA from cell line 14266, from which RNA was extracted after nucleus-cytoplasm fractionation.

Nuclear and cytoplasmic RNA were prepared, according to published protocols (64), by incubating 10 million cells in 1 ml of lysis buffer (10 mM Tris-HCl, pH 7.4; 150 mM NaCl, 1.5 mM $MgCl_2$, 100 mM NaF, 10 ng/ml aprotinin, 1 mM PMSF, 1 mM DTT, 10 U/ml RNasin, and 0.5% NP-40) for 15 minutes on ice. Cells were disrupted by passing them through hypodermic needles (25 G) 10 times. The crude nuclear fraction for nuclear mRNA extraction was obtained by collecting the pellet after centrifugation at 1,000 *g* for 5 minutes at 4°C. The supernatant was centrifuged for a further 5 minutes at 11,500 *g* for 5 minutes at 4°C. The cytosolic RNA was extracted from the supernatant of this second centrifugation step.

To prepare mRNA-derived cDNA, 2 μg of RNA was retrotranscribed using anchored poly-dT oligos ($dT_{20}VN$) and Superscript III reverse transcriptase (Invitrogen) and followed by RNase H treatment to remove RNA. For pre-mRNA analysis, RNA was treated with RNase-free DNAse I (Roche) to completely remove the DNA and was retrotranscribed using random hexamers. To confirm the absence of genomic DNA in cDNA preparations, control reactions lacking the reverse transcriptase enzyme (–RT) were performed. These preparations were run in parallel to and used as negative controls for each RT-PCR or real-time PCR amplification.

*Semiquantitative RT-PCR*. We consulted the Entrez Gene database for sequence information (http://www.ncbi.nlm.nih.gov; mRNA and protein sequences of PRPF31, NM_015629 and NP_056444, respectively; mRNA and protein sequences of UPF1, NM_002911.3 and NP_002902.2, respectively). Specific primer pairs were designed to amplify regions of the cDNA containing all mutations studied (Supplemental Table 2). To detect the c.319C>G mutation, a supplementary primer specific to the mutant allele was designed to distinguish between the different alleles. Specific primers were also designed to detect all 3 different forms of *PRPF31* cDNA resulting from the c.1115_1125del mutation, i.e., wild-type and long and short mutant forms.

PCR conditions and primer sequences were optimized for each primer set to amplify only the targeted nucleic acid species (e.g., mature RNA or pre-mRNA), including cycling conditions that were determined to be within the linear phase of the amplification. PCRs were performed in a final reaction volume of 25 μl containing 1× HotStart Taq PCR buffer, 500 μM $MgCl_2$, 100 μM 2′-deoxynucleoside 5′-triphosphate mix, 200 nM of each primer, and 0.1 U of HotStart Taq (QIAGEN). Reactions were incubated at 95°C for 15 minutes followed by 35 cycles at 95°C for 15 seconds and at 60°C for 1 minute. For primer pairs that amplified the cDNA carrying the c.319C>G, c.856-2A>G, or c.877_910del mutations, 1× Q-Solution (QIAGEN) was added to the reaction mix, and the PCR conditions were modified as follows: 95°C for 15 minutes followed by 35 cycles at 95°C for 15 seconds and at 62.6°C for 1 minute.

PCR products were resolved on 3% Nusieve 3:1 agarose gels (Cambrex) and by capillary electrophoresis with the eGene HDA-GT12 Multi-Channel Genetic Analyzer (eGene Inc.) and quantified by 2 independent methods, i.e., by using ImageJ software (65) on agarose gels and by using Biocalculator software (eGene Inc.) for runs performed with the HDA-GT12 instrument. Data obtained with these 2 methods were combined to calculate the mean values of the ratio between mutant and wild-type band intensities, and the error propagation relative to this operation was calculated accordingly. An exception to this method was for measurements performed in carriers of the c1115_1125del mutation, because agarose gel migration could not effectively separate the wild-type and the mutant mRNA long form and allow the proper use of the ImageJ software. Measurements for this mutation were obtained by using only the Biocalculator software.

To confirm the identity of the amplified products, and to generate size controls for all mutant and wild-type alleles, PCR products were subcloned into TOPO TA vectors (Invitrogen), purified with the Qiaprep Spin Miniprep Kit (Qiagen), and sequenced using the BigDye Terminator v1.1 Cycle Sequencing kit (Applied Biosystems).

*Real-time PCR*. Real-time PCRs were performed using the ABI Prism 7500 Sequence Detector in a final volume of 20 μl containing Power SybrGreen (Applied Biosystems) and using specific primers (Supplemental Table 2). As template, we used 4 μl of cDNA corresponding to 20 ng of retrotranscribed RNA.

Allele-specific real-time PCR for pre-mRNA allelic quantification in 3 patients with the c.1115_1125del mutation was performed using primers specific to either the wild-type or mutant pre-mRNA (Supplemental Table 2). Further allele-specific real-time PCR primer pairs were designed to quantify the nuclear and cytoplasmic long mutant mRNA form molecules versus the wild-type mRNA, in the presence or absence of NMD inhibitors, in carriers of the c.1115_1125del mutation and for mutant versus wild-type mRNA alleles from the positive control cell line 14266 (Supplemental Table 2). These allele-specific quantifications were performed by using the "standard curve" method, using the wild-type pre-mRNA or mRNA expression as a reference and

the mutant pre-mRNA or long-form mRNA expression as a target. To determine the amplification efficiency of each allele, standard curves were generated by interpolating wild-type and mutant Ct values obtained from serial dilutions of pooled cDNA and from dilutions of plasmids containing either the mutant or the corresponding wild-type cloned fragment (1- to 250-fold range over 5 points, for all curves). Amplification efficiencies were confirmed to be identical for both the cDNA and the plasmid templates. Quantification standards were generated as follows: known ratios of plasmids containing the mutant or wild-type cloned fragments were mixed (wild-type/mutant, 90:10, 80:20, 70:30, 60:40, and 50:50), their Ct values were determined, and their corresponding amounts (in terms of dilution units) were calculated by interpolation from the relevant standard curve. These reference values were then used to normalize the experimentally obtained amounts of wild-type and mutant alleles present in a given cell line, expressed as the relative amount of *PRPF31* mutant pre-mRNA or long-form mRNA with respect to *PRPF31* wild-type pre-mRNA or mRNA.

Non-allele–specific real-time PCR was performed to quantify nuclear *PRPF31* pre-mRNA after actinomycin D treatment by using the 18S ribosomal RNA gene (Gen Bank access M10098.1) as an endogenous control. Relative quantification of the amount of *PRPF31* pre-mRNA was again calculated by using the "standard curve" method. Standard curves for *PRPF31* pre-mRNA and 18S RNA were generated via 5 serial dilutions over a 250-fold range using a pool of cDNA samples to be analyzed. Individual Ct values from each gene were interpolated from the relevant standard curve, and the amount of *PRPF31* pre-mRNA for each time point was quantified relative to 18S RNA.

*Antibodies and quantitative Western blotting*. To detect both full-length and potential truncated PRPF31 proteins, anti PRPF31 antibodies were raised in rabbits against the N-terminal peptide sequence SLADELLADLEEAA; the serum was affinity purified using a peptide column containing the same residues (Eurogentec). This antibody was reactive against recombinant N-terminal His-tagged PRPF31 and, as previously described for PRPF31 (32), specifically detected a single 61-kDa protein band from total HeLa cell extracts (data not shown).

Total protein was extracted from lymphoblastoid cell lines derived from patients in RIPA buffer (150 mM NaCl, 50 mM Tris-HCl, pH 7.4; 1 mM EDTA, 1% Tx-100, 0.1% SDS, and 0.5% sodium deoxycholate) plus Complete mini EDTA-free protease inhibitor tablets (Roche). The total protein content was estimated using the BCA Protein Assay Kit (Pierce), and equal amounts were run on denaturing SDS-PAGE gels with Precision Prestained Protein Standards (Bio-Rad). Proteins were transferred to nitrocellulose membrane (Millipore) using the Mini-Protean II western transfer apparatus (Bio-Rad). Membranes were blocked in 5% Blotto (5% w/v skim milk powder in PBS) for 1 hour at room temperature. Primary antibody incubations were performed for 1 hour at room temperature using polyclonal anti-PRPF31 (1:500) or monoclonal anti–β-actin (1:2,500; Sigma-Aldrich), and washes were performed in 0.1% Tween-20 in PBS. Mouse and rabbit antibodies were detected simultaneously in 2 channels using fluorescently labeled secondary antibodies (IRDye800 donkey anti-rabbit IgG; IRDye680 donkey anti-mouse IgG) according to the manufacturer's instructions (LI-COR Biosciences). Bands were visualized and intensity analyzed using the Odyssey Infra-Red Detector and associated analysis software (LI-COR Biosciences).

*Indirect immunofluorescence*. Cultured lymphoblasts were washed with PBS and attached to 0.01% poly-L-lysine–treated coverslips, followed by methanol fixation for 5 min at –20°C and rehydration in PBS for 5 min at room temperature. Blocking and antibody incubations were performed in 5% normal swine serum, and washes were performed in 0.2% Tx-100 in PBS. Specific proteins were detected using affinity-purified rabbit antibody raised against the C-terminal residues of PRPF31 (1:500 dilution) (32), colocalized with mouse anti-SC35 (1:750; Sigma-Aldrich). Following 3 washes for 5 min, primary antibodies were visualized using fluorescently conjugated anti-rabbit Alexa 594 or anti-mouse Alexa 488 (Molecular Probes) at a dilution of 1:200. Slides were washed a further 3 times for 5 min, and the nuclei were stained with VectaShield Mounting Medium plus DAPI (Vector Labs) for 3 min followed by one wash for 5 min. Slides were mounted using Mowiol Mounting Medium (Calbiochem), and staining was visualized under an Axioskop 40 epifluorescent microscope (Carl Zeiss MicroImaging Inc.) and using associated analysis software (Axiovision; Carl Zeiss MicroImaging Inc.).

*Statistics*. Statistical comparison between 2 sets of data was performed using a 2-tailed Student's *t* test. A *P* value less than 0.05 was considered significant.

## Acknowledgments

We thank Reinhard Lührmann and Cindy Will for the C-terminal anti-PRPF31 antibody used for immunofluorescence and Goranka Tanackovic for helpful scientific discussions. This work was supported by Swiss National Science Foundation grant 310000-109620, by funds from the SVS (Sciences, Vie, Société) Program, by the Foundation Fighting Blindness, and by National Eye Institute grant EY00169 (to E.L. Berson).

Received for publication October 12, 2007, and accepted in revised form January 9, 2008.

Address correspondence to: Carlo Rivolta, Department of Medical Genetics, University of Lausanne, Rue du Bugnon 27, 1005 Lausanne, Switzerland. Phone: 41-21-692-5456; Fax: 41-21-692-5455; E-mail: carlo.rivolta@unil.ch.

1. Berson, E.L. 1993. Retinitis pigmentosa. The Friedenwald Lecture. *Invest. Ophthalmol. Vis. Sci.* **34**:1659–1676.
2. Berson, E.L., et al. 1993. A randomized trial of vitamin A and vitamin E supplementation for retinitis pigmentosa. *Arch. Ophthalmol.* **111**:761–772.
3. Berson, E.L., et al. 2004. Further evaluation of docosahexaenoic acid in patients with retinitis pigmentosa receiving vitamin A treatment: subgroup analyses. *Arch. Ophthalmol.* **122**:1306–1314.
4. Rivolta, C., Sharon, D., DeAngelis, M.M., and Dryja, T.P. 2002. Retinitis pigmentosa and allied diseases: numerous diseases, genes, and inheritance patterns. *Hum. Mol. Genet.* **11**:1219–1227.
5. Hartong, D.T., Berson, E.L., and Dryja, T.P. 2006. Retinitis pigmentosa. *Lancet.* **368**:1795–1809.
6. Daiger, S.P., and University of Texas Health Science Center. 2007. RetNet: genes and mapped loci causing retinal diseases. http://www.sph.uth.tmc.edu/RetNet/disease.htm.
7. Weidenhammer, E.M., Singh, M., Ruiz-Noriega, M., and Woolford, J.L. 1996. The PRP31 gene encodes a novel protein required for pre-mRNA splicing in Saccharomyces cerevisiae. *Nucleic Acids Res.* **24**:1164–1170.
8. Berson, E.L., Gouras, P., Gunkel, R.D., and Myrianthopoulos, N.C. 1969. Dominant retinitis pigmentosa with reduced penetrance. *Arch. Ophthalmol.* **81**:226–234.
9. Waseem, N.H., et al. 2007. Mutations in the gene coding for the pre-mRNA splicing factor, PRPF31, in patients with autosomal dominant retinitis pigmentosa. *Invest. Ophthalmol. Vis. Sci.* **48**:1330–1334.
10. Vithana, E.N., et al. 2001. A human homolog of yeast pre-mRNA splicing gene, PRP31, underlies autosomal dominant retinitis pigmentosa on chromosome 19q13.4 (RP11). *Mol. Cell.* **8**:375–381.
11. McKie, A.B., et al. 2001. Mutations in the pre-mRNA splicing factor gene PRPC8 in autosomal dominant retinitis pigmentosa (RP13). *Hum. Mol. Genet.* **10**:1555–1562.
12. Chakarova, C.F., et al. 2002. Mutations in HPRP3, a third member of pre-mRNA splicing factor genes, implicated in autosomal dominant retinitis pigmentosa. *Hum. Mol. Genet.* **11**:87–92.
13. Keen, T.J., et al. 2002. Mutations in a protein target of the Pim-1 kinase associated with the RP9 form of autosomal dominant retinitis pigmentosa. *Eur. J. Hum. Genet.* **10**:245–249.
14. Hentze, M.W., and Kulozik, A.E. 1999. A perfect message: RNA surveillance and nonsense-mediated decay. *Cell.* **96**:307–310.
15. Chang, Y.F., Imam, J.S., and Wilkinson, M.F. 2007. The nonsense-mediated decay RNA surveillance pathway. *Annu. Rev. Biochem.* **76**:51–74.
16. Holbrook, J.A., Neu-Yilik, G., Hentze, M.W., and Kulozik, A.E. 2004. Nonsense-mediated decay approaches the clinic. *Nat. Genet.* **36**:801–808.
17. Khajavi, M., Inoue, K., and Lupski, J.R. 2006. Nonsense-mediated mRNA decay modulates clinical

outcome of genetic disease. *Eur. J. Hum. Genet.* **14**:1074–1081.
18. Hall, G.W., and Thein, S. 1994. Nonsense codon mutations in the terminal exon of the beta-globin gene are not associated with a reduction in beta-mRNA accumulation: a mechanism for the phenotype of dominant beta-thalassemia. *Blood.* **83**:2031–2037.
19. Wang, L., et al. 2003. Novel deletion in the pre-mRNA splicing gene PRPF31 causes autosomal dominant retinitis pigmentosa in a large Chinese family. *Am J. Med. Genet. A.* **121**:235–239.
20. Martinez-Gimeno, M., et al. 2003. Mutations in the pre-mRNA splicing-factor genes PRPF3, PRPF8, and PRPF31 in Spanish families with autosomal dominant retinitis pigmentosa. *Invest. Ophthalmol. Vis. Sci.* **44**:2171–2177.
21. Xia, K., et al. 2004. A novel PRPF31 splice-site mutation in a Chinese family with autosomal dominant retinitis pigmentosa. *Mol. Vis.* **10**:361–365.
22. Lu, S.S., et al. 2005. Novel splice-site mutation in the pre-mRNA splicing gene PRPF31 in a Chinese family with autosomal dominant retinitis pigmentosa [In Chinese]. *Zhonghua Yan Ke Za Zhi.* **41**:305–311.
23. Sato, H., et al. 2005. Mutations in the pre-mRNA splicing gene, PRPF31, in Japanese families with autosomal dominant retinitis pigmentosa. *Am. J. Ophthalmol.* **140**:537–540.
24. Abu-Safieh, L., et al. 2006. A large deletion in the adRP gene PRPF31: evidence that haploinsufficiency is the cause of disease. *Mol. Vis.* **12**:384–388.
25. Sullivan, L.S., et al. 2006. Genomic rearrangements of the PRPF31 gene account for 2.5% of autosomal dominant retinitis pigmentosa. *Invest. Ophthalmol. Vis. Sci.* **47**:4579–4588.
26. Chakarova, C.F., et al. 2006. Molecular genetics of retinitis pigmentosa in two Romani (Gypsy) families. *Mol. Vis.* **12**:909–914.
27. Sullivan, L.S., et al. 2006. Prevalence of disease-causing mutations in families with autosomal dominant retinitis pigmentosa: a screen of known genes in 200 families. *Invest. Ophthalmol. Vis. Sci.* **47**:3052–3064.
28. Rivolta, C., et al. 2006. Variation in retinitis pigmentosa-11 (PRPF31 or RP11) gene expression between symptomatic and asymptomatic patients with dominant RP11 mutations. *Hum. Mutat.* **27**:644–653.
29. Taira, K., Nakazawa, M., and Sato, M. 2007. Mutation c. 1142 del G in the PRPF31 gene in a family with autosomal dominant retinitis pigmentosa (RP11) and its implications. *Jpn. J. Ophthalmol.* **51**:45–48.
30. Vithana, E.N., Chakarova, C., Patel, R.J., and Bhattacharya, S.S. 2004. Can the stability of a mutant mRNA copy of PRPF31 with an 11bp deletion be compromised through alternative splicing [abstract]? *Invest. Ophthalmol. Vis. Sci.* **45**:2484.
31. Moore, A.T., et al. 1993. Autosomal dominant retinitis pigmentosa with apparent incomplete penetrance: a clinical, electrophysiological, psychophysical, and molecular genetic study. *Br. J. Ophthalmol.* **77**:473–479.
32. Makarova, O.V., Makarov, E.M., Liu, S., Vornlocher, H.P., and Luhrmann, R. 2002. Protein 61K, encoded by a gene (PRPF31) linked to autosomal dominant retinitis pigmentosa, is required for U4/U6*U5 tri-snRNP formation and pre-mRNA splicing. *EMBO J.* **21**:1148–1157.
33. Schaffert, N., Hossbach, M., Heintzmann, R., Achsel, T., and Luhrmann, R. 2004. RNAi knockdown of hPrp31 leads to an accumulation of U4/U6 di-snRNPs in Cajal bodies. *EMBO J.* **23**:3000–3009.
34. Qian, L., Vu, M.N., Carter, M.S., Doskow, J., and Wilkinson, M.F. 1993. T cell receptor-beta mRNA splicing during thymic maturation in vivo and in an inducible T cell clone in vitro. *J. Immunol.* **151**:6801–6814.
35. Noensie, E.N., and Dietz, H.C. 2001. A strategy for disease gene identification through nonsense-mediated mRNA decay inhibition. *Nat. Biotechnol.* **19**:434–439.
36. Kim, Y.K., Furic, L., Desgroseillers, L., and Maquat, L.E. 2005. Mammalian Staufen1 recruits Upf1 to specific mRNA 3'UTRs so as to elicit mRNA decay. *Cell.* **120**:195–208.
37. Paillusson, A., Hirschi, N., Vallan, C., Azzalin, C.M., and Muhlemann, O. 2005. A GFP-based reporter system to monitor nonsense-mediated mRNA decay. *Nucleic Acids Res.* **33**:e54.
38. Zufferey, R., Nagy, D., Mandel, R.J., Naldini, L., and Trono, D. 1997. Multiply attenuated lentiviral vector achieves efficient gene delivery in vivo. *Nat. Biotechnol.* **15**:871–875.
39. Anczukow, O., et al. 2007. Does the nonsense-mediated mRNA decay mechanism prevent the synthesis of truncated BRCA1, CHK2, and p53 proteins? *Hum. Mutat.* **29**:65–73.
40. Usuki, F., et al. 2004. Inhibition of nonsense-mediated mRNA decay rescues the phenotype in Ullrich's disease. *Ann. Neurol.* **55**:740–744.
41. Deramaudt, B.M., Inglehearn, C.F., and Pierce, E.A. 2005. Haploinsufficiency of Prpf8 does not cause retinal degeneration [abstract]. *Invest. Ophthalmol. Vis. Sci.* **46**:5263.
42. Graziotto, J., Inglehearn, C.F., and Pierce, E.A. 2005. Characterization of pre-RNA processing factor 3 (Prpf3) knock-out mice [abstract]. *Invest. Ophthalmol. Vis. Sci.* **46**:5262.
43. Graziotto, J.J., Inglehearn, C.F., and Pierce, E.A. 2006. Characterization of pre-RNA processing factor 3 (Prpf3) knockin mice [abstract]. *Invest. Ophthalmol. Vis. Sci.* **47**:4588.
44. Graziotto, J.J., Inglehearn, C.F., and Pierce, E.A. 2007. Characterization of compound knockin Prpf3/Prpf8 mice [abstract]. *Invest. Ophthalmol. Vis. Sci.* **48**:3002.
45. Vithana, E.N., et al. 2003. Expression of PRPF31 mRNA in patients with autosomal dominant retinitis pigmentosa: a molecular clue for incomplete penetrance? *Invest. Ophthalmol. Vis. Sci.* **44**:4204–4209.
46. Pedersen, A.G., and Nielsen, H. 1997. Neural network prediction of translation initiation sites in eukaryotes: perspectives for EST and genome analysis. *Proc. Int. Conf. Intell. Syst. Mol. Biol.* **5**:226–233.
47. Li, S., Leonard, D., and Wilkinson, M.F. 1997. T cell receptor (TCR) mini-gene mRNA expression regulated by nonsense codons: a nuclear-associated translation-like mechanism. *J. Exp. Med.* **185**:985–992.
48. Brown, K.D., et al. 1997. The ataxia-telangiectasia gene product, a constitutively expressed nuclear protein that is not up-regulated following genome damage. *Proc. Natl. Acad. Sci. U. S. A.* **94**:1840–1845.
49. Moolman, J.A., et al. 2000. A newly created splice donor site in exon 25 of the MyBP-C gene is responsible for inherited hypertrophic cardiomyopathy with incomplete disease penetrance. *Circulation.* **101**:1396–1402.
50. Schollen, E., et al. 2007. Characterization of two unusual truncating PMM2 mutations in two CDG-Ia patients. *Mol. Genet. Metab.* **90**:408–413.
51. Khan, S.G., et al. 2006. Reduced XPC DNA repair gene mRNA levels in clinically normal parents of xeroderma pigmentosum patients. *Carcinogenesis.* **27**:84–94.
52. Matsuura, S., et al. 2006. Monoallelic BUB1B mutations and defective mitotic-spindle checkpoint in seven families with premature chromatid separation (PCS) syndrome. *Am. J. Med. Genet. A.* **140**:358–367.
53. Lee, W.C., et al. 2006. Suppression of galactosylceramidase (GALC) expression in the twitcher mouse model of globoid cell leukodystrophy (GLD) is caused by nonsense-mediated mRNA decay (NMD). *Neurobiol. Dis.* **23**:273–280.
54. Zhang, R.Z., et al. 2002. Effects on collagen VI mRNA stability and microfibrillar assembly of three COL6A2 mutations in two families with Ullrich congenital muscular dystrophy. *J. Biol. Chem.* **277**:43557–43564.
55. You, K.T., et al. 2007. Selective translational repression of truncated proteins from frameshift mutation-derived mRNAs in tumors. *PLOS Biol.* **5**:e109.
56. Deery, E.C., et al. 2002. Disease mechanism for retinitis pigmentosa (RP11) caused by mutations in the splicing factor gene PRPF31. *Hum. Mol. Genet.* **11**:3209–3219.
57. Liu, S., et al. 2007. Binding of the human Prp31 Nop domain to a composite RNA-protein platform in U4 snRNP. *Science.* **316**:115–120.
58. Mordes, D., et al. 2007. Identification of photoreceptor genes affected by PRPF31 mutations associated with autosomal dominant retinitis pigmentosa. *Neurobiol. Dis.* **26**:291–300.
59. Yuan, L., Kawada, M., Havlioglu, N., Tang, H., and Wu, J.Y. 2005. Mutations in PRPF31 inhibit pre-mRNA splicing of rhodopsin gene and cause apoptosis of retinal cells. *J. Neurosci.* **25**:748–757.
60. Linde, L., et al. 2007. Nonsense-mediated mRNA decay affects nonsense transcript levels and governs response of cystic fibrosis patients to gentamicin. *J. Clin. Invest.* **117**:683–692.
61. Bateman, J.F., Freddi, S., Nattrass, G., and Savarirayan, R. 2003. Tissue-specific RNA surveillance? Nonsense-mediated mRNA decay causes collagen X haploinsufficiency in Schmid metaphyseal chondrodysplasia cartilage. *Hum. Mol. Genet.* **12**:217–225.
62. Al Maghtheh, M., et al. 1994. Identification of a sixth locus for autosomal dominant retinitis pigmentosa on chromosome 19. *Hum. Mol. Genet.* **3**:351–354.
63. Rajavel, K.S., and Neufeld, E.F. 2001. Nonsense-mediated decay of human HEXA mRNA. *Mol. Cell. Biol.* **21**:5512–5519.
64. Corbin, F., et al. 1997. The fragile X mental retardation protein is associated with poly(A)+ mRNA in actively translating polyribosomes. *Hum. Mol. Genet.* **6**:1465–1472.
65. Abramoff, M.D., Magelhaes, P.J., and Ram, S.J. 2004. Image processing with ImageJ. *Biophotonics Int.* **11**:36–42.